HHS Public Access

Author manuscript

Pediatr Res. Author manuscript; available in PMC 2018 August 30.

Published in final edited form as:

Pediatr Res. 2013 June ; 73(6): 756–762. doi:10.1038/pr.2013.45.

Quantification of white matter injury following neonatal stroke with serial DTI

Niek E van der Aa[1], **Frances J. Northington**[2], **Brian S. Stone**[2,3], **Floris Groenendaal**[1], **Manon J.N.L. Benders**[1], **Giorgio Porro**[4], **Shoko Yoshida**[5,6], **Susumu Mori**[5,6], **Linda S. de Vries**[1], and **Jiangyang Zhang**[5]

[1]Department of Neonatology, Wilhelmina Children's Hospital, University Medical Center, Utrecht, The Netherlands [2]Department of Pediatrics, Eudowood Neonatal Pulmonary Division-NICN, Johns Hopkins University School of Medicine, Baltimore, MD, USA [3]Department of Neonatology, Children's National Medical Center, Washington, DC, USA [4]Department of Ophthalmology, University Medical Center Utrecht, The Netherlands [5]Dept. of Radiology, Johns Hopkins University School of Medicine, Baltimore, MD, USA [6]F.M. Kirby Functional Imaging Center, Kennedy Krieger Institute, Baltimore, MD, USA

Abstract

Background: Diffusion tensor imaging (DTI) can be used to predict outcome following perinatal arterial ischemic stroke (PAIS), though little is known about white matter changes over time.

Methods: Infants with PAIS were serially scanned in the neonatal period (n=15), at 3 months (n=16), and at 24 months (n=8). FA-values in five regions of interest (anterior and posterior limb of the internal capsule, corpus callosum, optic radiation and posterior thalamic radiation) were obtained and compared with FA- values of healthy controls and **neurodevelopmental outcome**.

Results: In the neonatal period, no differences in FA were found. At three months, **the six** infants who ultimately developed motor deficits showed lower FA-values in all affected regions. Four infants developed a visual field defect and showed lower FA-values in the affected optic radiation at three months **(0.22 vs 0.29,p=0.03)**. **Finally, a correlation between FA-values of the corpus callosum at three months and the Griffiths's developmental quotients was found (*r* =.66 p=0.03). At 24 months a similar pattern was observed.**

Conclusion: Neonatal FA measurements may underestimate the extent of injury following PAIS. FA measurements at three months could be considered a more reliable predictor of neurodevelopmental outcome and correlate with DTI findings at 24 months.

Corresponding Author: Frances J. Northington, MD PhD, frances@jhmi.edu, Johns Hopkins University, Neonatology Research Lab, 600 N. Wolfe Street, CMSC 6-104, Baltimore, MD 21287, Tel: (410) 502-6794, Fax: (410) 614-8388.

Disclosures:
Besides the financial support, the authors have nothing to disclose.

Introduction:

Perinatal arterial ischemic stroke (PAIS), with an incidence of 1 per 2300–4000 live births, often leads to adverse neurologic sequelae (1, 2). Currently there are no accepted therapies for the acute treatment of PAIS, but methods to accurately predict later neurodevelopmental outcome in the first few months following PAIS are rapidly advancing. Magnetic resonance imaging (MRI) plays an important role in the diagnosis of PAIS and the subsequent prognosis of motor development (3–9).

Several cross sectional studies have reported **differences** in diffusion tensor imaging (DTI) parameters following PAIS. **Beyond the neonatal** period, decreased integrity of the affected corticospinal tracts, reflected by lower fractional anisotropy (FA) values, has been observed in children who developed motor deficits (7, 8, 10). However, no studies have reported longitudinal measurements using DTI following PAIS. In preterm born infants, longitudinal studies have provided insight in both structural and functional development and have identified windows for therapeutic intervention (11, 12). Aim of the current study therefore was to examine the potential value of serial DTI following PAIS to evaluate temporal changes of white matter injury and **to** determine the optimal strategy to predict outcome following PAIS.

Methods:

Patient selection and Neurodevelopmental Assessment

Sixteen **full** term infants (11 male, median gestational age 40 weeks, range $37^{2/7}$ – $41^{3/7}$) cared for in the neonatal intensive care unit at the Wilhelmina Children's Hospital, who were diagnosed with PAIS and underwent cranial MRI during the first week after birth were included in this retrospective study. **In 15 of these infants, DTI data were acquired during the neonatal period.** Strokes were observed in the territories of the posterior cerebral artery (PCA, n=3) and middle cerebral artery (MCA, n=13). One infant's MRI showed **a main trunk MCA stroke on T2, without diffusion restriction, suggesting an antenatal onset of approximately 7–10 days before birth.**

No permission is required from the institutional review board for this type of study. Informed parental consent was obtained before each MRI scan. Eleven of the included infants were previously studied as part of a larger cohort, in which DTI-based tractography of the corticospinal tracts was performed at the age of three months (8).

A second MRI was obtained at a median age of 3.4 months (range 2.9–4.4 months) in all children and eight children were scanned again at a median age of 23.2 months (range 16.4–29.6 months). Neurodevelopmental outcome was evaluated at **between 18 and 36 months** using the Griffiths' mental developmental scale **(Hogrefe, Oxford, UK)**. Presence of unilateral motor deficits (UMD) was assessed according to Claeys (13).

In the infants in whom development of a visual field defect was thought to be likely due to involvement of the optic radiation, cortex or thalamus, an experienced pediatric ophthalmologist performed visual field examinations. This could be done from the age of

three months onwards with the BEFIE test (*be*havioural visual *fie*ld testing) (14). **In this test, the examiner stands behind the child and rotates an arc with a ball attached to its tip around the child's head, from the periphery to the centre of the visual field. The angle at which the child first detects the stimulus determines the borders of the visual field.** The visual fields were subsequently scored as normal, presence of a quandrantanopia or presence of a hemianopia.

DTI protocol

Patients were scanned on a 1.5T Philips MR scanner (Philips Medical Systems, Best, The Netherlands) using a SENSE head coil. The neonatal and three months DTI protocol consisted of a single-shot EPI sequence (EPI factor 43, TR/TE 6817/87 ms) with 50 axial 2 mm slices in 32 non-collinear diffusion-weighted directions with a b-value of 800 s/mm^2 and one b=0 s/mm^2 image (field of view 190×190 mm, acquisition matrix 96×96, reconstruction matrix 128×128). At 2 years a similar single-shot EPI sequence was used but with an EPI factor of 51, a TR of 8382ms and field of view of 192×192 mm.

During the first two scans, infants were sedated as described previously (8). A vacuum pillow (Med-Tec, Orange City, IA) was used to prevent head movement. Minimuffs (Natus Medical Inc, San Carlos, CA) were used for hearing protection and a neonatologist was present throughout the exam. At two years, children received general anaesthesia, were ventilated and the heart rate, ventilation and transcutaneous oxygen saturation were **monitored** by an anaesthetist.

Control subjects

DTI scans of 42 healthy children (age 0–30 months) were used to create reference curves for the different regions of interest (ROIs) and to create age-matched templates. These data were obtained from a database of normative scans, which were acquired on a 1.5T Philips MR scanner at Johns Hopkins Univeristy (15).

Image Post Processing

Images were processed with ExploreDTI (www.exploredti.com). The diffusion-weighted images were realigned to the b0-image to correct for subject motion and eddy current induced geometric distortions. In this process, the diffusion tensor was fitted for each voxel after adjusting the diffusion gradients for the b-matrix rotation (16). After this procedure, the mean diffusion weighted image (mDWI), the b0 image, and the fractional anisotropy (FA) image were exported for further analysis. Finally, the brain volume was extracted manually by removing signals in the mDWI images from tissues outside the brain (skull-stripping).

Next, the DTI data were normalized to a single subject neonatal DTI template, consisting of a mDWI, FA and b0 image, which are freely available (cmrm.med.jhmi.edu). The mDWI image of each subject was aligned with the mDWI of the template using a 12-mode affine transformation provided by the automated image registration software (Figure 1) (17). This transformation was then applied to the FA images and followed by dual contrast (FA and mDWI) large deformation diffeomorphic metric mapping (LDDMM) as provided by the Diffeomap software (www.mristudio.org), using descending alphas of 0.05, 0.04 and 0.03 to

achieve coarse-to-fine normalization (18, 19). In infants with a large middle cerebral artery (MCA) stroke, the extensive high signal intensity on the mDWI and the subsequent cyst at three months hindered accurate normalization. In these infants, the LDDMM at 0 month was driven by the b0 and FA images. At three months, the LDDMM was preceded by a landmark-based LDDMM with approximately 180–200 landmarks to bring structures displaced by the cyst close to their normal locations as in the template (20). The result was further improved by a single alpha (0.05) dual-contrast LDDMM, and visually inspected to ensure accurate normalization for the major white matter tracts.

Region of interest-based analysis

After normalization of the controls to the template, FA values were determined in the normalized FA images using five regions of interest (ROIs) defined in the template image. These ROIs included the corpus callosum, the posterior and anterior limb of the internal capsule, the posterior thalamic radiation and the optic radiation. This procedure produced consistent definitions of ROIs among subjects. FA values of bilateral ROIs were averaged for each control and plotted against age. GraphPad Prism v5.0 (GraphPad Software, San Diego, CA) was used to fit FA values as a function of age of the controls, using an exponential regression model. The 95% and 99% prediction intervals were calculated for each ROI separately **(Supplemental Figure 1)**. FA values in these five ROIs were also determined for the patients and were plotted in the curves of the controls. **FA values of patients were regarded normal when they fell within the 95% prediction intervals and abnormal if they fell below the intervals.**

Maps of standard Z-scores

For each voxel in the template with an FA >0.2 an exponential fit was performed, fitting the FA values of the controls as a function of age using Matlab R2011a (Mathworks, Natick, MA). The mean FA and the standard error of each voxel were estimated at different ages from the exponential fitting and were used to calculate standard Z-scores with respect to the controls for each voxel as

$$Z = \frac{X_{patient} - \bar{X}_{control}}{SE}$$

where $X_{patient}$ is the FA value of the patient's voxel and $\bar{X}_{control}$ and SE are the mean FA and standard error of the control subjects at the voxel.

Statistical analysis

Differences in clinical parameters or FA values between groups were tested using the Mann-Whitney U test. The Bonferonni post hoc test was used for testing multiple ROI's at each time point. Spearman's correlation coefficient was used to determine the relation between the Griffiths' DQ and FA values.

RESULTS:

Patient outcome

The median follow-up duration was 37 months (range 19–62 months). Six children (five main trunk MCA, one anterior trunk MCA) developed UMD. The median Griffiths' DQ was 98 (range 81–105).

Visual field examinations were performed in ten children (63%), including all children with a PCA stroke or main trunk MCA stroke **and revealed a** visual field **defect** in four children (three main trunk MCA, one PCA stroke). **This included a hemianopia in two children and a quandrantanopia in two others.**

ROI analysis & motor outcome

On the first scan, acquired during the first week after birth, FA values in the ROIs in the affected hemisphere were not different from the reference values based from the controls. At this time, median FA values of infants who would later develop UMD did not differ from those who would not develop UMD (table 1). Only two infants with a main trunk MCA stroke, one of whom had an antenatal MCA stroke, already showed **abnormal** FA values in several regions in the affected hemisphere in the neonatal period (Figure 2A). One child with a PCA stroke, without subsequent development of UMD also showed **abnormal** FA values in the posterior thalamic radiation and optic radiation, which was still present at three months.

At 3 months, **FA values in the affected hemisphere of infants who would later develop UMD clearly started to deviate** from the reference values of controls in several ROIs. The FA values in all affected ROIs of these infants were also lower when compared to the corresponding FA values of the infants who did not develop UMD.

In the eight children who were also scanned at approximately 24 months, FA values which were below the 95% prediction interval at three months remained below this curve at 24 months (Figure 2B). The FA in the ROIs in the unaffected hemisphere of the children who developed UMD did not differ from the FA in the corresponding ROIs of the children who did not develop UMD at any time point **and all followed the reference curve**.

ROI analysis & visual fields

At three months, FA values of the affected optic radiation were lower in the infants who would later develop a visual field defect (0.22 vs 0.29, p=0.03) and were below the reference curve. In three infants of these infants, FA values were also abnormal on the neonatal scan (Figure 3). In the six children with a normal visual field, five showed normal FA values at three months. One child with a main trunk MCA stroke **showed** an **abnormal** FA value in the affected optic radiation at three months without a detectable visual field defect.

No visual field test was acquired in the six remaining children. There were however no anamnestic signs for a visual field defect in these children and the FA of their affected optic radiation was within the 95% prediction intervals at 3 months.

Finally, a correlation was observed between the Griffiths' DQ and the FA of the corpus callosum at the second scan (r =.66 p=0.03, **Supplemental Figure 2**). No correlation **between the Griffiths' DQ and** FA values of other ROIs was found at any time.

Maps of standard Z-scores

The z-maps showed similar findings as the ROI analysis. In an infant with a main trunk MCA stroke (**Figure 4**), where the neonatal scan showed no apparent abnormality in FA values, the 3 months scan clearly indicated a decreased FA in the posterior limb of the internal capsule and several white matter tracts. This spatial pattern was mostly preserved at the 24 months scan.

The z-maps also provide additional information, showing potential local abnormalities not detected in the ROI analysis. An example is the low FA value in the splenium of the corpus callosum in an infant with a PCA stroke (**Supplemental Figure 3**), while the FA value of the corpus callosum ROI was normal.

Discussion:

In the present study, serial DTI data of infants diagnosed with PAIS were acquired to examine the **temporal evolution of white matter injury and correlate this with neurodevelopmental outcome.** We were able to **demonstrate** time related changes in FA values in regions commonly affected by PAIS. **While neonatal FA values tended tocould underestimate the injury, FA values at three months tended to show the full extent of injury and** correlated **not only with the observed FA values at 24 months**, **but also** with long-term neurodevelopmental outcome

Little is known about the changes in FA during the first week following PAIS and both increased and decreased FA values have been reported following hypoxic-ischemic injury (21, 22). In adult stroke an initial increase of FA values is found, followed by a decrease from day five onwards (23). The initial increase is thought to reflect a reduced spacing between the axons due to the cytotoxic edema, while the subsequent loss of structural integrity results in a decrease in FA. This suggests that the timing of FA measurements **following stroke** is important, **which was also observed in the infant with the antenatal stroke. This infant most likely suffered a stroke 7–10 days before birth and already showed abnormal FA values on the neonatal scan, while such low FA values were not yet observed in the other infants who would later develop UMD.** FA measurements in the first week, during the acute phase, **therefore** seem to be of limited value, and need to be considered within the timing of the injury and with conventional MRI and DWI results.

At three months, clear differences in FA values could be observed, which corresponded with development of motor deficits, cognitive outcome and development of visual field defects. Even though this suggests that three months **is** a better time point to predict outcome using **FA measurements, DTI at this time can not replace neonatal imaging. During the neonatal period, conventional MRI and DWI remain essential for the diagnosis of PAIS and have also proven their value in predicting development of motor disabilities following PAIS (3, 4, 6, 9).** Conventional MRI and DWI, however, can not be

used to quantify the severity of white matter injury related to motor disabilities or visual field defects, as can be done using DTI, even before the development of clinical symptoms (8, 10). **We therefore propose that the place of DTI should be after the acute phase, i.e. after 4–6 weeks, to evaluate the extent of injury and predict neurodevelopmental outcome in infants at risk.**

Visual field defects following PAIS are not uncommon and have been reported in 20% of all cases (9). Prediction of visual field defects using conventional MRI is difficult as involvement of the optic radiation or visual cortex does not always result in deficits. In preterm born infants, DTI-based tractography of the optic radiation at term-equivalent age is associated with visual function (24). Though the number of children who underwent a visual field exam was restricted to those with larger lesions, our data suggest that FA measurements of the optic radiation at three months can predict visual field defects. Larger studies will be needed to confirm this finding and may differentiate between development of a hemianopia and quadrantanopia.

Using the z-maps, we were able to examine the spatial pattern of white matter injury in both the acute and post-acute phase. **This method allowed visualization of white matter integrity over time without the predefined ROIs.** Both preterm and term studies **have shown** that brain injury can result in widespread abnormalities of white matter development at sites remote from a focal lesion (28, 29). **In the current study this was also observed, e.g. in the corpus callosum and fornix (Figure 4).** The importance of widespread white matter injury is hard to overestimate because multiple defects in brain development including delayed/abnormal myelination, abnormal cortical folding, and decreased thalamic volume have been associated with global white matter injury in preterm infants (29) and these abnormalities almost certainly underlie the complex neurobehavioral deficits found in these children and similar findings are likely following PAIS.

Technical considerations

It is necessary to note that the control and patient images in this study were acquired using different scanners with different settings, which may have introduced a scanner dependent bias (30). Assessing such bias would require careful calibration of scanner instruments, on which no consensus has been reached yet. **However, the FA values determined in the ROIs in the unaffected hemisphere nicely followed the reference curve, suggesting that if any scanner dependent bias in FA values was present, it would be minimal.**

The reported results strongly depend on an accurate normalization of the data to the atlas. While LDDMM has been used before in older children with cerebral palsy (31), this paper is the first attempt to normalize images from infants with severe injury, e.g., the presence of a large ischemic lesion or cyst. For these cases, time-consuming landmark-based normalization, expert knowledge, and careful inspection are necessary to guarantee accurate normalization. **This procedure is therefore not yet suitable for daily clinical practice. Incorporation of automatic lesion segmentation techniques and masking of these regions during the registration process may bring this method a step closer to the clinician (32, 33).**

A limitation of the study was the relatively small sample size and the absence of a visual field test in six children. The data in this study were collected retrospectively and visual field tests we therefore only administered if clinically indicated.

Conclusion:

Serial DTI following PAIS allows insight in the evolution of white matter injury following PAIS. While neonatal DTI may not capture the full extent of injury, DTI at three months does, as it corresponds well with DTI findings at 24 months in major white matter tracts examined here and long-term motor and visual outcome. DTI at three months can therefore be considered an early predictor of outcome following PAIS **and may provide additional information to neonatal imaging.**

Supplementary Material

Refer to Web version on PubMed Central for supplementary material.

Acknowledgments

Financial support:

N.E. van der Aa was supported by grants from the Ter Meulen Foundation, Foundation ‘De Drie Lichten’, the Wilhelmina Children’s Research Foundation and the Dutch Phelps Foundation for this project. Further financial support was received from the March of Dimes Foundation (6–08-275) (Frances J Northington) and the National Institutes of Health NS 059529 (Jiangyang Zhang).

References

1. Nelson KB, Lynch JK 2004 Stroke in newborn infants. Lancet Neurol 3:150–158. [PubMed: 14980530]
2. Kirton A, deVeber G 2009 Advances in perinatal ischemic stroke. Pediatr.Neurol 40:205–214. [PubMed: 19218034]
3. Kirton A, Shroff M, Visvanathan T, deVeber G 2007 Quantified corticospinal tract diffusion restriction predicts neonatal stroke outcome. Stroke 38:974–980. [PubMed: 17272775]
4. de Vries LS, van der Grond J, van Haastert IC, Groenendaal F 2005 Prediction of outcome in newborn infants with arterial ischaemic stroke using diffusion-weighted magnetic resonance imaging. Neuropediatrics 36:12–20. [PubMed: 15776318]
5. Lee J, Croen LA, Lindan C, Nash KB, Yoshida CK, Ferriero DM, Barkovich AJ, Wu YW 2005 Predictors of outcome in perinatal arterial stroke: a population-based study. Ann Neurol 58:303–308. [PubMed: 16010659]
6. Husson B, Hertz-Pannier L, Renaud C, Allard D, Presles E, Landrieu P, Chabrier S 2010 Motor outcomes after neonatal arterial ischemic stroke related to early MRI data in a prospective study. Pediatrics 126:912–918. [PubMed: 20855393]
7. Roze E, Harris PA, Ball G, Elorza LZ, Braga RM, Allsop JM, Merchant N, Porter E, Arichi T, Edwards AD, Rutherford MA, Cowan FM, Counsell SJ 2012 Tractography of the corticospinal tracts in infants with focal perinatal injury: comparison with normal controls and to motor development. Neuroradiology 54:507–516. [PubMed: 22006424]
8. van der Aa NE, Leemans A, Northington FJ, van Straaten HL, van Haastert IC, Groenendaal F, Benders MJ, de Vries LS 2011 Does Diffusion Tensor Imaging-Based Tractography at 3 Months of Age Contribute to the Prediction of Motor Outcome After Perinatal Arterial Ischemic Stroke? Stroke 42:3410–3414. [PubMed: 22020032]

9. Mercuri E, Anker S, Guzzetta A, Barnett A, Haataja L, Rutherford M, Cowan F, Dubowitz L, Braddick O, Atkinson J 2003 Neonatal cerebral infarction and visual function at school age. Arch Dis Child Fetal Neonatal Ed 88:F487–491. [PubMed: 14602696]
10. Glenn OA, Ludeman NA, Berman JI, Wu YW, Lu Y, Bartha AI, Vigneron DB, Chung SW, Ferriero DM, Barkovich AJ, Henry RG 2007 Diffusion tensor MR imaging tractography of the pyramidal tracts correlates with clinical motor function in children with congenital hemiparesis. AJNR Am.J.Neuroradiol 28:1796–1802. [PubMed: 17893220]
11. Smyser CD, Inder TE, Shimony JS, Hill JE, Degnan AJ, Snyder AZ, Neil JJ 2010 Longitudinal analysis of neural network development in preterm infants. Cereb Cortex 20:2852–2862. [PubMed: 20237243]
12. Groppo M, Ricci D, Bassi L, Merchant N, Doria V, Arichi T, Allsop JM, Ramenghi L, Fox MJ, Cowan FM, Counsell SJ, Edwards AD 2012 Development of the optic radiations and visual function after premature birth. Cortex:10.1016/j.cortex.2012.1002.1008.
13. Claeys V, Deonna T, Chrzanowski R 1983 Congenital hemiparesis: the spectrum of lesions. A clinical and computerized tomographic study of 37 cases. Helv Paediatr Acta 38:439–455. [PubMed: 6668195]
14. Porro GJ, Hofmann J, Wittebol-Post D, van Nieuwenhuizen O, van der Schouw YT, Schilder MBH, Dekker MEM, Treffers WF 1998 A new behavioral visual field test for clinical use in pediatric neuro-ophthalmology. Neuro-opthalmology 19:205–214.
15. Hermoye L, Saint-Martin C, Cosnard G, Lee SK, Kim J, Nassogne MC, Menten R, Clapuyt P, Donohue PK, Hua K, Wakana S, Jiang H, van Zijl PC, Mori S 2006 Pediatric diffusion tensor imaging: normal database and observation of the white matter maturation in early childhood. Neuroimage. 29:493–504. [PubMed: 16194615]
16. Leemans A, Jones DK 2009 The B-matrix must be rotated when correcting for subject motion in DTI data. Magn Reson Med 61:1336–1349. [PubMed: 19319973]
17. Woods RP, Grafton ST, Holmes CJ, Cherry SR, Mazziotta JC 1998 Automated image registration: I. General methods and intrasubject, intramodality validation. J Comput Assist Tomogr 22:139–152. [PubMed: 9448779]
18. Miller MI, Trouve A, Younes L 2002 On the metrics and euler-lagrange equations of computational anatomy. Annu Rev Biomed Eng 4:375–405. [PubMed: 12117763]
19. Ceritoglu C, Oishi K, Li X, Chou MC, Younes L, Albert M, Lyketsos C, van Zijl PC, Miller MI, Mori S 2009 Multi-contrast large deformation diffeomorphic metric mapping for diffusion tensor imaging. Neuroimage 47:618–627. [PubMed: 19398016]
20. Joshi SC, Miller MI 2000 Landmark matching via large deformation diffeomorphisms. IEEE Trans Image Process 9:1357–1370. [PubMed: 18262973]
21. Ward P, Counsell S, Allsop J, Cowan F, Shen Y, Edwards D, Rutherford M 2006 Reduced fractional anisotropy on diffusion tensor magnetic resonance imaging after hypoxic-ischemic encephalopathy. Pediatrics 117:e619–630. [PubMed: 16510613]
22. van Pul C, Buijs J, Vilanova A, Roos FG, Wijn PF 2006 Infants with perinatal hypoxic ischemia: feasibility of fiber tracking at birth and 3 months. Radiology 240:203–214. [PubMed: 16709789]
23. Sotak CH 2002 The role of diffusion tensor imaging in the evaluation of ischemic brain injury - a review. NMR Biomed. 15:561–569. [PubMed: 12489102]
24. Bassi L, Ricci D, Volzone A, Allsop JM, Srinivasan L, Pai A, Ribes C, Ramenghi LA, Mercuri E, Mosca F, Edwards AD, Cowan FM, Rutherford MA, Counsell SJ 2008 Probabilistic diffusion tractography of the optic radiations and visual function in preterm infants at term equivalent age. Brain 131:573–582. [PubMed: 18222994]
25. van Kooij BJ, de Vries LS, Ball G, van Haastert IC, Benders MJ, Groenendaal F, Counsell SJ 2012 Neonatal tract-based spatial statistics findings and outcome in preterm infants. AJNR Am J Neuroradiol 33:188–194. [PubMed: 21998101]
26. Maneru C, Junque C, Salgado-Pineda P, Serra-Grabulosa JM, Bartres-Faz D, Ramirez-Ruiz B, Bargallo N, Tallada M, Botet F 2003 Corpus callosum atrophy in adolescents with antecedents of moderate perinatal asphyxia. Brain Inj 17:1003–1009. [PubMed: 14514451]

27. Schatz J, Buzan R 2006 Decreased corpus callosum size in sickle cell disease: relationship with cerebral infarcts and cognitive functioning. J Int Neuropsychol Soc 12:24–33. [PubMed: 16433941]

28. Ramenghi LA, Rutherford M, Fumagalli M, Bassi L, Messner H, Counsell S, Mosca F 2009 Neonatal neuroimaging: going beyond the pictures. Early Hum Dev 85:S75–77. [PubMed: 19793628]

29. Ment LR, Hirtz D, Huppi PS 2009 Imaging biomarkers of outcome in the developing preterm brain. Lancet Neurol 8:1042–1055. [PubMed: 19800293]

30. Huisman TA, Loenneker T, Barta G, Bellemann ME, Hennig J, Fischer JE, Il'yasov KA 2006 Quantitative diffusion tensor MR imaging of the brain: field strength related variance of apparent diffusion coefficient (ADC) and fractional anisotropy (FA) scalars. Eur Radiol 16:1651–1658. [PubMed: 16532356]

31. Faria AV, Hoon A, Stashinko E, Li X, Jiang H, Mashayekh A, Akhter K, Hsu J, Oishi K, Zhang J, Miller MI, van Zijl PC, Mori S 2011 Quantitative analysis of brain pathology based on MRI and brain atlases--applications for cerebral palsy. Neuroimage 54:1854–1861. [PubMed: 20920589]

32. Brett M, Leff AP, Rorden C, Ashburner J 2001 Spatial normalization of brain images with focal lesions using cost function masking. Neuroimage 14:486–500. [PubMed: 11467921]

33. Ghosh N, Yuan X, Turenius CI, Tone B, Ambadipudi K, Snyder EY, Obenaus A, Ashwal S 2012 Automated core-penumbra quantification in neonatal ischemic brain injury. J Cereb Blood Flow Metab.

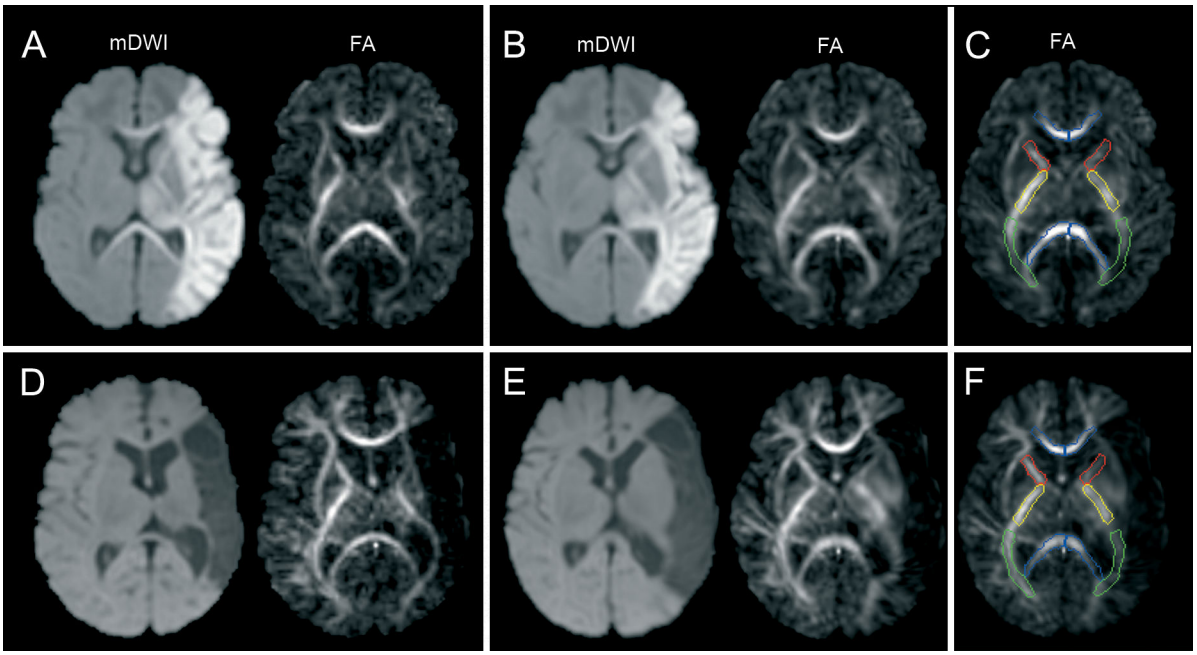

Figure 1.

Example of the normalization of two DTI datasets **acquired** in the neonatal period **(A-C)** and at the age of three months **(D-F)** in an infant with a **stroke** of the main trunk of the MCA. **After the affine registration (A,D) and subsequent LDDMM procedure (B,E) FA values were determined in the regions of interest (C,F).**

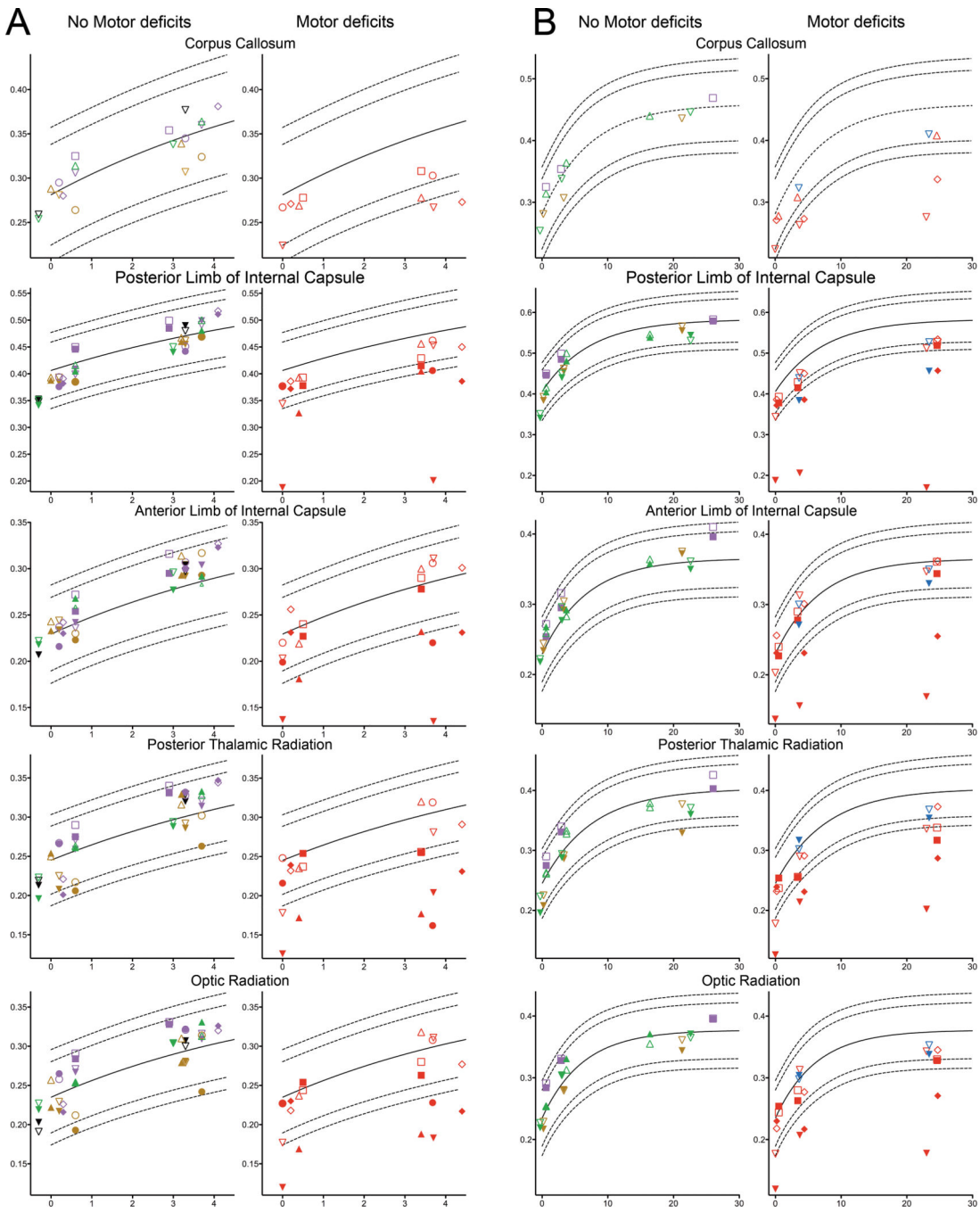

Figure 2:

The FA values (vertical axis) in the different ROIs versus the age at scan (horizontal axis) of 16 infants who were scanned in the neonatal period and at three months (A) and of the 8 infants who were also scanned at 24 months (B), **shown for infants with a normal motor development (left column) and with development of motor deficits (right column).** The FA value of the affected side is depicted as a filled symbol, while the unaffected side is depicted by the corresponding open symbol. For the corpus **callosum**, the mean FA was determined and depicted. The different colours represent the different kinds of strokes

observed: main branch MCA stroke (red), posterior branch MCA stroke (green), cortical MCA branch (purple), lenticulostriate branch MCA stroke (black) and PCA stroke (brown). The child with the antenatal MCA stroke is depicted as the upside down triangle. The dashed lines represent the 95% and 99% prediction intervals for each ROI, based on the controls.

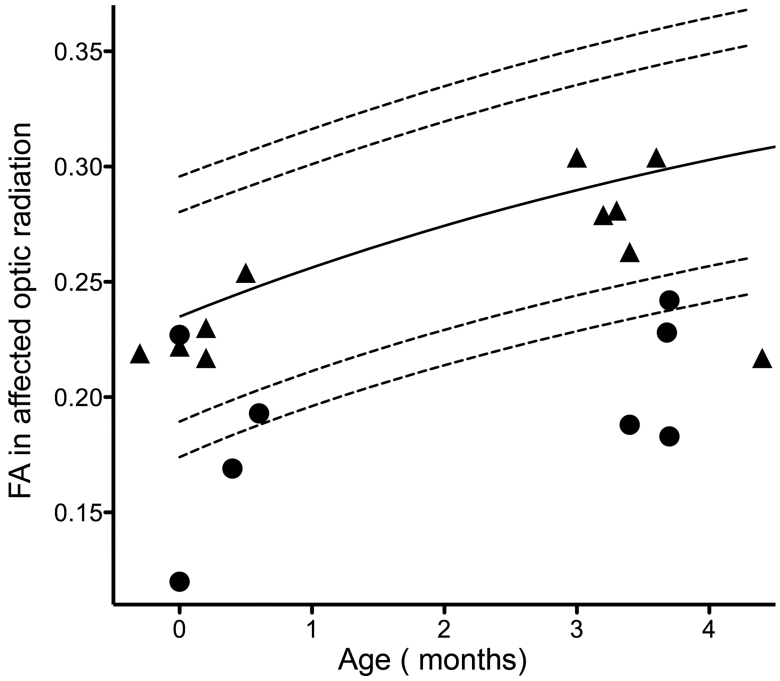

Figure 3:
FA values as determined in the affected optic radiation of the ten infants who were subsequently tested for visual field defects. The circles represent the infants who developed a visual field defect, while the triangles represent the infants with a normal visual field on follow-up.

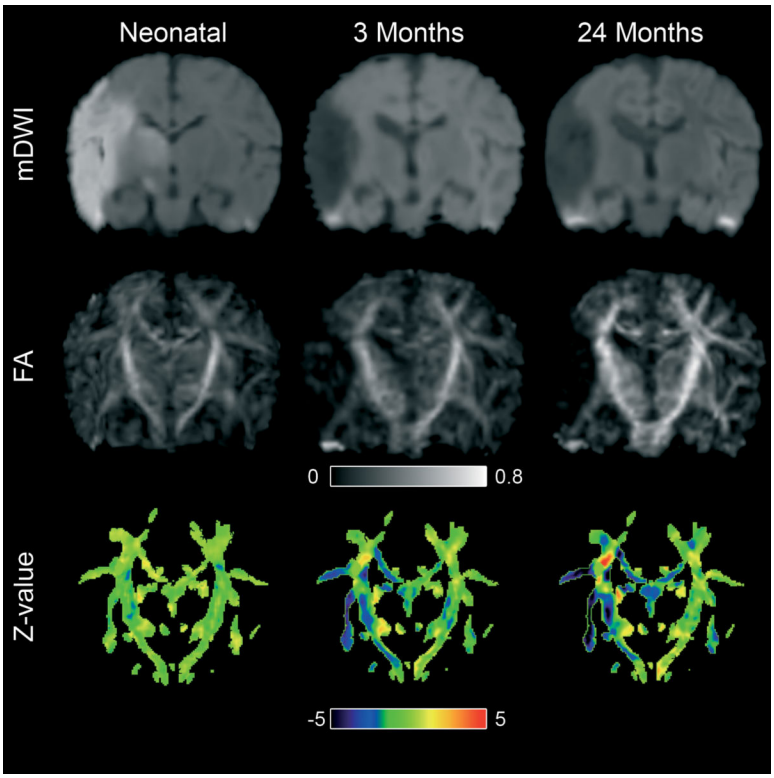

Figure 4:

Coronal views of serial DTI datasets after normalization to the template. The neonatal mDWI shows an ischemic area in the MCA territory, which resulted in a cyst as observed at 3 and 24 months. The neonatal Z-map shows a normal Z-value in all regions. At three months, low Z-values, representing abnormal FA values, can be observed in the affected corticospinal tract, which corresponded with the subsequent development of unilateral motor deficits. The Z-map at 24 months shows an almost identical image. Interestingly, FA values in the fornix showed continued decrease from neonatal to 24 months, suggesting delayed degeneration in this tract.

Table 1

Median FA values of the five different ROIs as measured in the infants who did develop motor deficits versus those who did not. In the neonatal period no significant differences were found between the two groups. At three months, significant differences were observed in all ROIs. These differences could still be observed at 24 months, but did no longer reach significance due to the smaller group of children scanned at 24 months.

	Neonatal DTI (n=15)	3 Months DTI (n=16)	24 Months DTI (n=8)
CC	.27 vs .28 **(*p*=0.55)**	.29 vs .35 **(*p*=0.03)**	.37 vs .44 **(*p*=0.10)**
PLIC	.37 vs .38 **(*p*=0.49)**	.40 vs .48 **(*p*=0.01)**	.46 vs .55 **(*p*=0.10)**
ALIC	.20 vs .23 **(*p*=0.55)**	.23 vs .29 **(*p*=0.02)**	.29 vs .36 **(*p*=0.41)**
OR	.22 vs .23 **(*p*=1.0)**	.22 vs .31 **(*p*=0.05)**	.30 vs .37 **(*p*=0.10)**
PTR	.22 vs .23 **(p=1.0)**	.22 vs .32 **(*p*=0.04)**	.31 vs .37 **(*p*=0.41)**